Catalysis Today 175 (2011) 106–111

Contents lists available at ScienceDirect

Catalysis Today

journal homepage: www.elsevier.com/locate/cattod

Catalytic performance of supported precious metal catalysts for the combustion of diesel particulate matter

Cheol-Beom Lim[a], Hajime Kusaba[b], Hisahiro Einaga[b], Yasutake Teraoka[b,*]

[a] Department of Molecular and Material Sciences, Interdisciplinary Graduate School of Engineering Sciences, Kyushu University, Kasuga, Fukuoka 816-8580, Japan
[b] Department of Energy and Material Sciences, Faculty of Engineering Sciences, Kyushu University, Kasuga, Fukuoka 816-8580, Japan

ARTICLE INFO

Article history:
Received 14 October 2010
Received in revised form 22 March 2011
Accepted 30 March 2011
Available online 17 May 2011

Keywords:
Diesel particulate matter
Soot
Soluble organic fraction
Supported precious metal catalysts

ABSTRACT

CeO_2 and TiO_2 supported precious metal (Ag, Pt and Pd) catalysts were prepared by an impregnation method, and their catalytic performance for oxidation of simulated diesel particulate matter (PM) was investigated by thermogravimetry (TG), differential thermal analysis (DTA) and mass spectrometry (MS) under both tight-contact (TC) and loose-contact (LC) conditions. The simulated PM was prepared by liquid-phase adsorption of SOF (eicosane, $C_{20}H_{42}$) on soot (carbon black). Catalytic performance for the oxidation of simulated PM depended on both metal species and supports. CeO_2 was inherently active for both SOF and soot oxidation, and TiO_2 was nearly inactive. Pt was the most active species for SOF oxidation, followed by Pd and Ag. The SOF oxidation was independent of contact condition between the simulated PM and catalysts. Soot oxidation performance, on the other hand, drastically affected by the contact conditions, and Ag was far more active than Pt and Pd under both TC and LC conditions. Ag/CeO_2 was the most active soot oxidation catalyst. The oxidation of soot was influenced by the coexisting SOF depending on catalytic materials and contact modes.

1. Introduction

Diesel engines have many advantages as compared with gasoline engines. For example, the combustion efficiency at high air/fuel ratio and fuel economy of diesel engines are superior to those of gasoline engines and emissions of CO and CO_2 gases from diesel engines are much lower than those of gasoline engines [1]. Recently, global warming has become serious environmental problem, and the emission of CO_2 gas is one of the critical causes for global warming. Therefore, the development of low CO_2 emission vehicles is strongly required and diesel vehicles are one of the most realistic alternatives to reduce CO_2 emission from vehicles. Furthermore, diesel engines are winning an increasing share of light duty vehicles and passenger cars [2]. However, the diesel engine exhausts harmful materials such as nitrogen oxides (NOx) and diesel particulate matter (PM), and PM is know to cause serious environmental and health problems [3,4]. Therefore, the strict regulations for PM emission are enforced in many advanced countries.

The development of PM removal technologies is highly required, and various technologies have been developed to control PM. The reduction technologies of PM emissions from diesel vehicles are classified as improvement of fuel quality, improvement of engine performance and development of diesel exhaust after-treatment system. The research has been ongoing with respect to the diesel exhaust after-treatment, and especially catalyst coated diesel particulate filter (DPF) system is the most effective technology to control PM emission [5–7].

The PM consists of primarily carbon (soot), upon which soluble organic fraction (SOF), sulfates and water are adsorbed [8,9]. The target materials to be catalytically removed are soot and SOF. The concentration ratio of soot and SOF is different with different engine operation condition [10]. The SOF can range approximately from 20% to 60% of total PM composition and its concentration becomes the highest at light engine loads when exhaust temperature is low. The non-catalytic (spontaneous) oxidation temperature of diesel PM depends somehow on the SOF content but usually exceed 550 °C [11]. Catalysis can lead to a significant reduction in PM oxidation temperature, and therefore many researches have focused on the development of catalysts for efficient PM oxidation in DPF system. Most of these researches, however, have been focused on catalysts for only soot oxidation, and therefore the oxidation of SOF in PM and the effect of SOF on the soot oxidation should be investigated to understand the catalysis for real PM removal.

Among many catalyst components for soot oxidation, the most promising formulation is based on the addition of potassium to the oxides of transition metals (e.g. Cu, V, Mo, Co and Fe) [12–18], or perovskite-type catalysts such as $La_{1-x}K_xMnO_3$, $La_{0.7}Ag_{0.3}MnO_3$, $La_{1-x}Ce_xNiO_3$ and $LaMn_{0.7}Ni_{0.3}O_3$ [19–22]. Perovskite-type catalysts have been intensively investigated, because they have thermal

* Corresponding author. Tel.: +81 92 583 7526; fax: +81 92 583 8853.
E-mail address: teraoka@mm.kyushu-u.ac.jp (Y. Teraoka).

0920-5861/$ – see front matter © 2011 Elsevier B.V. All rights reserved.
doi:10.1016/j.cattod.2011.03.062

stability, low cost and potential of simultaneous removal of soot and nitrogen oxides (NOx).

Recently, precious metal supported catalysts (such as Ag on CeO_2 and γ-Al_2O_3) have been reported as active soot oxidation catalysts [23–26]. Ag is known to be an efficient partial oxidation catalyst, and the potential of Ag for the oxidation of carbon particle has been reported [23–26]. CeO_2 has the potential to accelerate the oxidation rate of soot due to active oxygen production [27–29]. According to the precedent studies, CeO_2-based mixed oxides (e.g. $MnO_X/CO_3O_4/ZrO_2/CuO–CeO_2$) have high potential for accelerating soot oxidation [30–33].

In order to understand the catalytic oxidation behavior of PM under the real condition, the catalytic oxidation of SOF and soot should be investigated. The aim of this work is to reveal the combustion characteristics of simulated PM which contained both SOF and soot. In this study, Ag, Pt, and Pd catalysts supported on TiO_2 and CeO_2 were prepared. Their catalytic performance for simulated PM was investigated under tight-contact and loose-contact condition.

2. Experimental

2.1. Catalysts preparation

Precious metal catalysts (Ag, Pt and Pd) supported on TiO_2 and CeO_2 catalysts were prepared by an impregnation method from aqueous solutions containing appropriate amounts of precious metal sources; silver nitrate (Kishida Chemical), diammine dinitro platinum(II) (Kojima Chemicals, HNO_3 solution) and palladium(II) nitrate (N.E.CHEMCAT, 5% aqueous solution). The loading of precious metals was 5 wt%. TiO_2 (JRC-TIO-4, $S_{BET} = 54\ m^2\ g^{-1}$) and CeO_2 (JRC-CEO-3, $S_{BET} = 86\ m^2\ g^{-1}$) were supplied from Catalysis Society of Japan. TiO_2 or CeO_2 powder was suspended in an aqueous solution of a metal precursor and evaporated-to-dryness under stirring. The obtained precursors were dried in heating oven at 100 °C for 20 h, followed by calcination in air at 700 °C for 5 h. TiO_2 and CeO_2 calcined under the same condition were used as the catalysts without precious metal loading. The crystal phases were characterized by XRD using Cu Kα radiation (Rigaku, RINT2200) and the specific surface area was determined by BET method from N_2 adsorption isotherm at 77 K (BELSORP-mini, BEL JAPAN, Inc.).

2.2. Preparation of simulated PM

Carbon black (CB, Sigma–Aldrich) and eicosane ($C_{20}H_{42}$, Tokyo Kasai) were used as substitutes for soot and SOF, respectively. Simulated PM was prepared by liquid-phase adsorption of eicosane on CB. The weight ratio of CB and eicosane was 3:2. CB was suspended in an n-hexane solution of eicosane (30 mL). The solvent completely evaporated after 45 min-stirring at room temperature, and the simulated PM was obtained.

2.3. PM combustion performance

Tight-contact (TC) and loose-contact (LC) mixtures of a catalyst and the simulated PM (*ca.* 5 wt%) were used. A catalyst and PM were well mixed in an agate mortar for 10 min and lightly mixed by spatula for 10 min to prepare TC and LC mixtures, respectively. The TC and LC mixtures of a catalyst and pure CB (*ca.* 5 wt%) were also used to investigate the effect of SOF on soot oxidation.

Thermogravimetry (TG) and differential thermal analysis (DTA) measurements (Shimadzu, DTG-60) were carried out for analysis of the catalytic oxidation of PM. The catalyst/PM mixture was heated at a rate of 10 °C min^{-1} from 30 °C to 800 °C in a flow of synthetic air (21% O_2 and 79% N_2, 100 mL min^{-1}). Mass spectrometer (MS) (Pfeifer Vacuum Quadrupol, OmniStar) was used to detect CO_2 ($m/e = 44$) in the effluent gas from the TG/DTA apparatus. The catalytic activity for soot oxidation was evaluated by the temperature (T_{max}) at which the slope (rate) of the weight loss due to the soot oxidation was the highest. T_{max} was determined from the peak-top of the derivative TG curve.

Table 1
Catalytic activity of precious metal supported TiO_2 catalysts for soot oxidation.

Catalyst	Specific surface area/$m^2\ g^{-1}$	T_{max}/°C			
		Simulated PM (CB + eicosane)		Soot (CB)	
		TC mode	LC mode	TC mode	LC mode
Ag/TiO_2	7.2	393	573	400	516
Pt/TiO_2	9.8	534	646	553	649
Pd/TiO_2	11.2	521	645	541	637
TiO_2	11.3	566	645	567	648

3. Results and discussion

3.1. Characterization of prepared catalysts

Fig. 1 shows the XRD patterns of CeO_2 and TiO_2-supported precious metal catalysts and specific surface areas of prepared catalysts are listed in Tables 1 and 2. Characteristic XRD peaks of the rutile phase were observed for TiO_2-based catalysts. As-received TiO_2 was a mixture of anatase (major) and rutile (minor) phases with 54 $m^2\ g^{-1}$ of specific surface area, and the complete transformation to rutile phase, which was accompanied with the reduction of the specific surface area to 11.3 $m^2\ g^{-1}$, took place during the calcination at 700 °C for 5 h. Crystalline phases of Ag, Pt and PdO were observed for TiO_2-supported catalysts. Specific surface areas were 11.2, 9.8 and 7.2 $m^2\ g^{-1}$ for Pd/TiO_2, Pt/TiO_2 and Ag/TiO_2, respectively. In the case of CeO_2-based catalysts in which CeO_2 crystallized in cubic fluorite structure, XRD peaks characteristic to precious metal species were observed not in Pd/CeO_2 but in Ag/CeO_2 and Pt/CeO_2, indicating that Pd species were highly dispersed on CeO_2. Specific surface areas of CeO_2-supported catalysts were 63 (CeO_2), 61 (Pd/CeO_2), 60 (Pt/CeO_2) and 38 (Ag/CeO_2) $m^2\ g^{-1}$.

3.2. PM oxidation performance

3.2.1. PM oxidation performance test by TG/DTA/MS

The simulated PM consisted of 40 wt% of SOF (eicosane) and 60 wt% of soot (CB). In the TG experiment in which a mixture of PM (5 wt%) and catalyst (95 wt%) were used, weight losses originated in SOF and soot should be 2 wt% and 3 wt% within a weighting error, respectively.

Fig. 2 shows representative results of PM oxidation measured by (A) TG, (B) DTA and (C) MS techniques when the tight-contact (TC) mixtures of simulated PM and catalysts (TiO_2, Pt/TiO_2 and

Table 2
Catalytic activity of precious metal supported CeO_2 catalysts for soot oxidation.

Catalyst	Specific surface area/$m^2\ g^{-1}$	T_{max}/°C			
		Simulated PM (CB + eicosane)		Soot (CB)	
		TC mode	LC mode	TC mode	LC mode
Ag/CeO_2	38	393	541	415	528
Pt/CeO_2	60	434	637	471	629
Pd/CeO_2	61	446	639	465	628
CeO_2	63	417	638	448	616

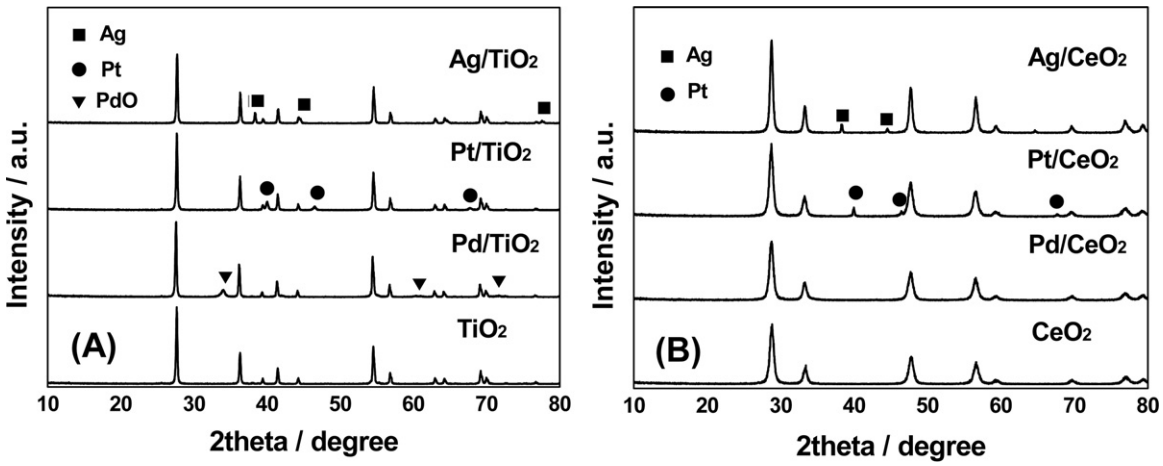

Fig. 1. XRD patterns of (A) TiO_2-based and (B) CeO_2-based catalysts with and without 5 wt% loading of Ag, Pt and Pd.

CeO_2) were heated at a rate of 10 °C min^{-1} in air. A set of TG and DTA curves for the catalyst was measured simultaneously, and the MS result was obtained by a separate run. Two weight loss steps were observed roughly below (first step) and above (second step) 300 °C.

General features of the temperature programmed oxidation of simulated PM by TG as a central method are first discussed. The weight losses at the first and second steps for TiO_2 and Pt/TiO_2 catalysts were about 2 and 3 wt% (Fig. 2(A)), and therefore they were reasonably ascribed to weight losses of SOF and soot, respectively. Considering the reactivity of SOF (hydrocarbon) and soot (carbon), this assignment could be accepted. In the temperature range of the first step, an exothermic peak which is a sign of the occurrence of the oxidation of SOF was observed with Pt/TiO_2 but not with bare TiO_2 (Fig. 2(B)). The formation of CO_2 was confirmed with Pt/TiO_2 and practically no CO_2 formation was observed with TiO_2 (Fig. 2(C)). These results clearly show that SOF (eicosane) in the simulated PM is oxidized on Pt/TiO_2 and that it desorbed or evaporated from the mixture before undergoing oxidation. Shapes of DTA and CO_2 formation curves of Pt/TiO_2 catalyst were almost the same; onset temperature was around 90 °C and after forming a plateau peak up to 175 °C, a sharp peak was observed around 190 °C. The TG curve with CeO_2 at the first step was different from those with TiO_2-based catalysts. The apparent differences were the appearance of weight increase peak with a maximum around 155 °C, extension of the step to higher temperature and the weight loss larger than 2 wt% (2.35 wt% loss at 275 °C). When natural coal which contained SOF was heated in an oxygen-containing atmosphere in TG apparatus, a weight increase was observed just before the steep weight loss due to combustion [34]. FT-IR investigation revealed that aliphatic C–H, which was detected in the original coal, was disappeared and instead aliphatic C=O was generated when the weight of the coal increased [34]. It can thus be reasonably inferred that the weight increase observed with CeO_2 can be ascribable to the partial oxidation of SOF to oxygenated compounds. Since peak tops of TG weight loss, DTA curve and CO_2 formation curve were almost the same, CO_2 formation and addition of oxygen to SOF molecules (oxygenation), which are accompanied with the weight loss and increase respectively, occurred simultaneously, and the latter event predominantly proceeded over the former when weight increased. DTA curve gave the peak around 155 °C, and a shoulder peak continued to about 300 °C. The shape of CO_2 formation curve was somewhat different from that of DTA curve, but appearance of two peaks, one at 155 °C and another up to 300 °C, was consistent with the DTA result. The weight loss at the first step which was larger than that expected might mean that a part of soot is oxidized in this step. As described above, SOF was oxidized by Pt/TiO_2 below 200 °C, and when the catalyst was inactive, SOF desorbed up to 200 °C without undergoing oxidation as in the case of TiO_2. Over CeO_2, on the other hand, SOF molecules partially oxidized to oxygenates, which probably suppresses desorption. The oxidation of oxygenates at temperatures higher than that of SOF oxidation might induce the oxidation of a part of neighboring soot.

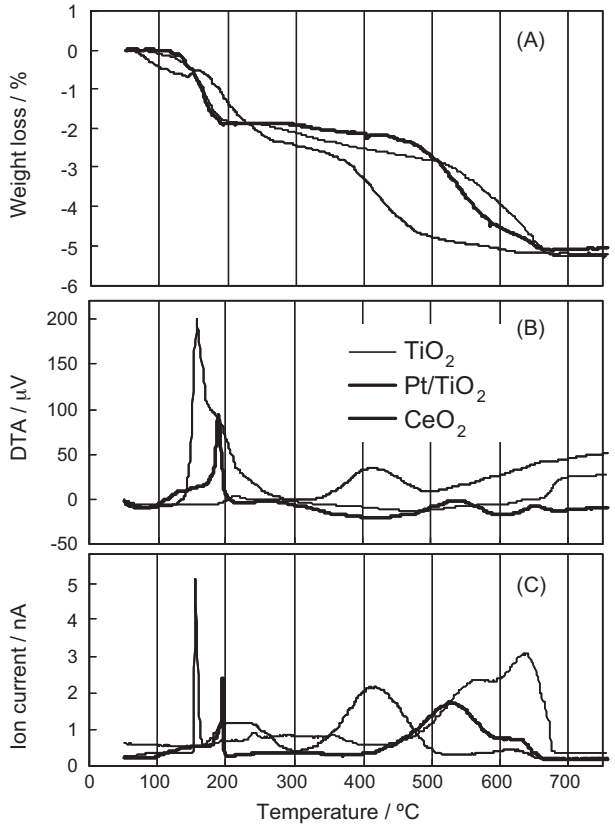

Fig. 2. Temperature programmed oxidation of tight mixture of simulated PM (CB + eicosane) and catalysts (Pt/TiO_2, TiO_2, CeO_2) measured by (A) TG, (B) DTA and (C) MS by tracing CO_2 ($m/e = 44$).

The second weight loss step originated from the oxidation of soot. For CeO_2, weight loss, DTA peak and CO_2 formation were observed around 420 °C. Observed with Pt/TiO_2 were two peaks

in both DTA and MS results and corresponding TG curves with inflection around 600 °C.

From experimental point of view, the activity for soot oxidation can be evaluated by TG and optionally DTA even when simulated PM is used. For the behavior of SOF in simulated PM, on the other hand, careful analysis of TG and DTA results is necessary because SOF undergoes direct oxidation to CO_2, partial oxidation to oxygenates and desorption. Combined use of MS with TG/DTA of course gives more precise information. In the following sections, PM oxidation property of precious metal catalysts loaded on TiO_2 and CeO_2 will be discussed, and the results shown in Fig. 2 clearly suggest that CeO_2 and TiO_2 are active and inactive support for PM oxidation, respectively. It has been reported that CeO_2 accelerate the oxidation of soot [27–29] because it carries active oxygen species at the surface and in the sub-surface region. The oxidation ability seems to be related more or less with the oxygen storage property by the redox between Ce^{4+} and Ce^{3+}. On the other hand, the reduction of TiO_2 is more difficult than that of CeO_2; the electrochemical standard reduction potentials at 298 K are +1.61 and 0.00 V for Ce^{4+}/Ce^{3+} and Ti^{4+}/Ti^{3+} pairs, respectively. Therefore, TiO_2 with less reducibility or redox ability is almost inactive for the oxidation of the simulated PM under the present experimental condition.

3.2.2. TiO_2 supported precious metal catalysts

TG/DTA results of mixtures of the simulated PM and TiO_2-based catalysts under TC and LC conditions are shown in Fig. 3(A) and (B), respectively. TG curves in the first weight-loss region were almost the same irrespective of catalysts and contact modes, while those in the second weight-loss region, that is, oxidation of soot, changed with catalysts and contact conditions. As described in Section 3.2.1, SOF underwent oxidation on Pt/TiO_2 and desorption on TiO_2 under the TC condition. The occurrence of oxidation of SOF was confirmed with Pd/TiO_2 catalyst by the appearance of a DTA peak, while desorption of SOF with disappearance of DTA peaks took place on Ag/TiO_2 catalyst. Judging from the position of DTA peaks, Pt/TiO_2 was more active than Pd/TiO_2 for the SOF oxidation.

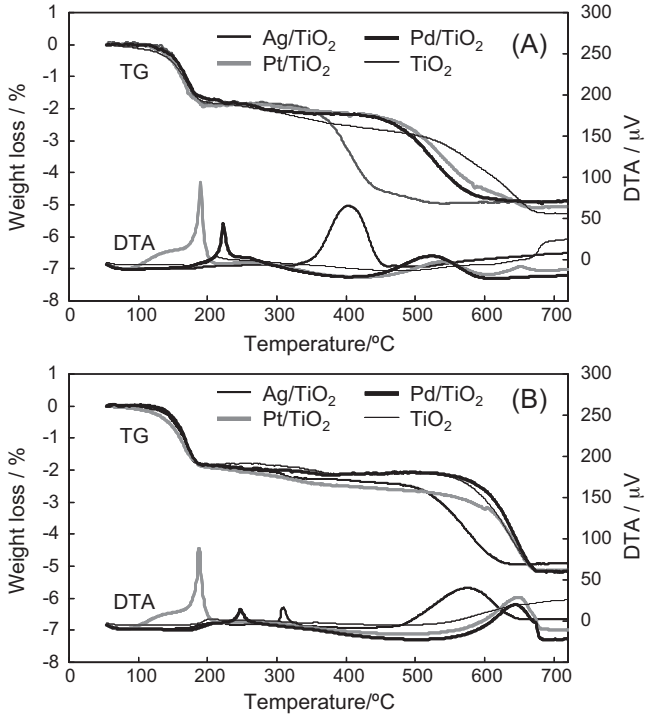

Fig. 3. TG and DTA curves of simulated PM (CB + eicosane) mixed with the TiO_2-based catalysts. (A) TC mode, (B) LC mode.

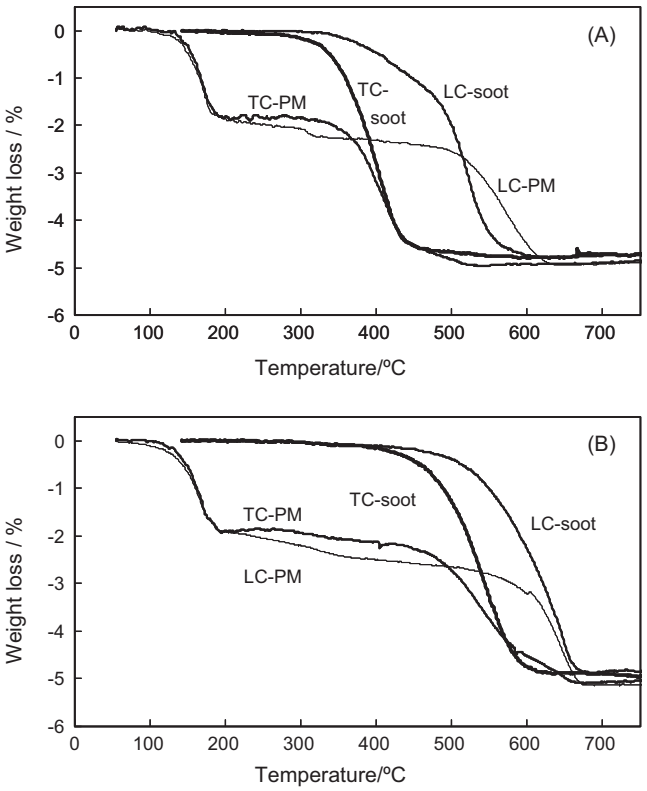

Fig. 4. TG curves of simulated PM and pure soot mixed with (A) Ag/TiO_2 and (B) Pt/TiO_2 under TC and LC conditions. Measurements were started around 50 and 150 °C for simulated PM and pure soot, respectively.

Ag/TiO_2 was less active than those two catalysts. It is noted that the absence of the exothermic peak does not necessarily mean the inertness of Ag against SOF oxidation, because in the present experimental method, desorption of SOF might occur below the temperature at which Ag becomes active for SOF oxidation. Almost the same position and shape of DTA peaks in TC and LC mixtures suggested that SOF oxidation on Pt/TiO_2 catalyst was independent of contact condition between the catalyst and simulated PM.

In the case of soot oxidation, on the other hand, the activity was greatly influenced by the contact condition. Under both TC and LC conditions, Ag/TiO_2 exhibited higher catalytic activity than Pt/TiO_2 and Pd/TiO_2, which is completely opposite to the activity order for SOF oxidation. The activities for the soot oxidation (T_{max}) on TiO_2-supported metal catalysts are summarized in Table 1. Here, T_{max} is the temperature at which the slope (rate) of the second weight loss due to the soot oxidation is the highest. For all the catalysts, T_{max} under TC condition were lower than those under LC condition. In both contact modes, Ag/TiO_2 showed the highest activity. Differences in T_{max} between Ag/TiO_2 and TiO_2 were 173 and 72 °C under TC and LC conditions, respectively. For Pt/TiO_2 and Pd/TiO_2, T_{max} under LC condition were practically the same as that with bare TiO_2, and differences in T_{max} from TiO_2 under the TC condition were 32 and 45 °C, respectively. It is inferred that Pt and Pd on TiO_2 show a weak catalytic activity under TC condition and no catalytic activity under LC condition for soot oxidation.

The effect of coexisting SOF on the soot oxidation was investigated by comparing TG curves of the simulated PM and pure soot. TG curves in the presence of Ag/TiO_2 and Pt/TiO_2 catalysts are shown in Fig. 4 as representative examples and T_{max} for all the cases are listed in Table 1. At temperature of soot oxidation, SOF originally present in the simulated PM was absent, but the oxidation of soot left was influenced by the catalysts and contact modes.

In the case of Ag/TiO_2 (Fig. 4(A)), soot in the simulated PM (PM-soot) was oxidized at nearly the same temperature in the TC mixture and at higher temperature in the LC mixture, as compared with oxidation of pure soot. As described above, SOF was not oxidized but desorbed from the mixture when Ag/TiO_2 catalyst was used. Since SOF molecules are adsorbed on the surface of soot, desorption of SOF brings about thinning (reduction of volume) of simulated PM, leaving core PM-soot. It is likely that the contact condition between Ag/TiO_2 and PM-soot becomes looser after desorption of SOF and therefore the oxidation of PM-soot takes place at higher temperature. This phenomenon is expected to have a remarkable influence in the LC mixture. In the TC mixture, however, its influence might be negligibly small because the simulated PM and PM-soot after the SOF desorption are present in close proximity to the catalyst.

For the Pt/TiO_2 catalyst (Fig. 4(B)), PM-soot and pure soot under the LC condition was oxidized at nearly the same temperature ((T_{max}; 646 °C (PM-soot), 649 °C (pure soot)). Under the TC condition, on the other hand, PM-soot (T_{max} = 534 °C) was oxidized at lower temperature than pure soot (T_{max} = 553 °C). The behavior of Pd/TiO_2 was close to that of Pt/TiO_2: PM-soot was oxidized at lower and similar temperatures under TC and LC conditions, respectively, as compared with pure soot. There results clearly indicate that the oxidation of PM-soot in the TC mixture with Pt/TiO_2 and Pd/TiO_2 catalysts proceeds easier than that of pure soot. Since SOF was not desorbed but oxidized with these catalysts, the oxidation event of SOF must bring about the promotion of PM-soot oxidation. One possibility is that surface of soot is activated during the SOF oxidation by, for example, the formation of oxygen-containing groups such as carboxylate and carbonyl groups which are more easily oxidized than surface carbon atoms. This event, if occurs, might promote the catalytic oxidation of soot under the TC condition, but have little influence under the LC condition because the catalyst is too remote from the soot to exert catalytic function. This is consistent with the above-mentioned results that Pt and Pd on TiO_2 show a weak catalytic activity under TC condition and no catalytic activity under LC condition for soot oxidation.

T_{max} values of PM-soot and pure soot with TiO_2 without precious metal were almost the same in each TC and LC condition, probably because soot oxidation mixed with inert TiO_2 is close to the spontaneous combustion of soot which occurs in the heterogeneous reaction field with the presence of an inert material.

The effect of the amount of PM mixed with Pt/TiO_2 catalyst on SOF and PM-soot oxidation was investigated under the LC condition (Fig. 5). Although T_{max} of PM-soot oxidation increased with increasing PM content from 1 wt% (632 °C) to 3 and 5 wt% (647 and 646 °C), the effect of PM loading on T_{max} was not so prominent, probably because T_{max} with Pt/TiO_2 under LC condition is close to that of spontaneous combustion of soot. Exothermic peaks of SOF oxidation were observed in all the cases. The onset temperature of DTA signal was around 90 °C irrespective of the PM loading amount, but the position of sharp peaks tended to increase as PM content increased. The identical onset temperature can be understood because it reflects the intrinsic catalytic activity of Pt on TiO_2 for SOF oxidation. Shape and peak position of DTA curve depend on how the exothermic reaction proceeds. When the amount of SOF is little like 1 wt%, SOF in PM is oxidized immediately after the ignition. With more amount of SOF, on the other hand, it takes time to complete oxidation of SOF and therefore the position of DTA peak shifts to higher temperature.

3.2.3. CeO_2 supported precious metal catalysts

Fig. 6 shows TG/DTA curves of simulated PM mixed with the CeO_2-supported precious metal catalysts under both TC and LC conditions. Two weight loss steps originated in SOF and soot were clearly observed. Strong and complicated exothermic peaks at the

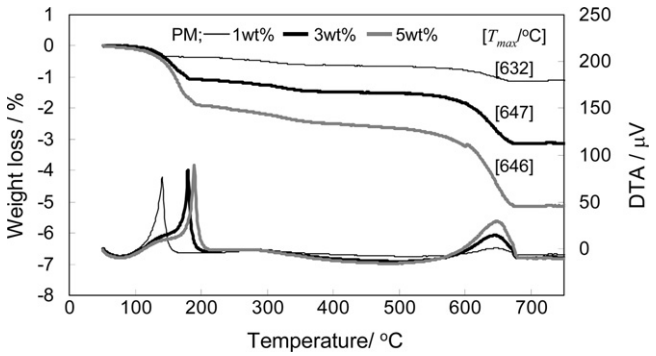

Fig. 5. TG and DTA curves of simulated PM with different mixing amount (1, 3 and 5 wt%) with Pt/TiO_2 catalyst under LC mode.

first step were observed for all the catalysts under TC and LC conditions. The full understanding of DTA peaks with complicated shapes is not straightforward, because it suggests that the complicated reactions take place. Therefore, effect of the catalysts on SOF oxidation is discussed mainly from the onset temperature of DTA signal under TC condition. It is noted that, judging from temperature range of the first step, SOF oxidation was nearly independent on contact conditions.

As explained in Section 3.2.1, CeO_2 had oxidation ability of SOF. The onset temperature with Ag/CeO_2 was identical to that with CeO_2, indicating that Ag on CeO_2 is inactive for SOF oxidation. DTA signals with CeO_2 and Ag/CeO_2 consisted of two peaks, and the intensity of the low temperature peak was stronger and weaker for CeO_2 and Ag/CeO_2, respectively. This might mean that SOF oxidation on CeO_2 proceeds more effectively than that on Ag/CeO_2 because of the larger specific surface area of CeO_2 ($63\ m^2\ g^{-1}$) than Ag/CeO_2 ($38\ m^2\ g^{-1}$). Lower onset temperature with Pt/CeO_2 and Pd/CeO_2 as compared with CeO_2 indicated that Pt and Pd on CeO_2 exhibited catalytic activity for SOF oxidation. The onset temperatures under TC condition were around 90 °C (Pt/TiO_2), 120 °C

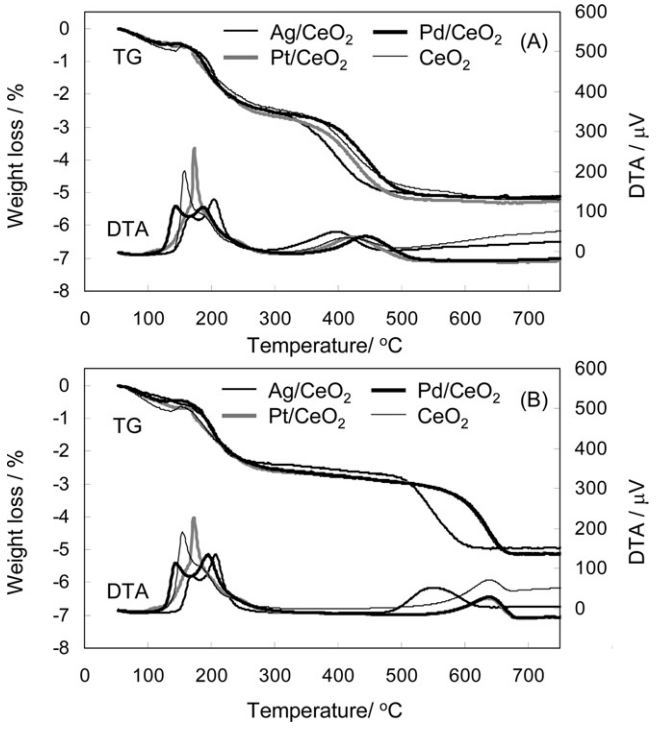

Fig. 6. TG and DTA curves of simulated PM (CB + eicosane) mixed with the CeO_2-based catalysts. (A) TC mode, (B) LC mode.

(Pd/TiO_2) and 50 °C (Pt/CeO_2 and Pd/CeO_2). The lower onset temperatures for CeO_2 supported catalysts indicate that Pd and Pt on CeO_2 are more active for SOF oxidation that those on TiO_2. The prominent increase in activity of Pd, which was more remarkable than that of Pt, probably related with the high dispersion of Pd on CeO_2 (Section 3.1).

It is clearly observed from Fig. 6 and Table 2 that Ag/CeO_2 was the most active for PM-soot oxidation under both TC and LC conditions. As in the case of TiO_2 supported catalysts, Pt and Pd on CeO_2 showed a weak catalytic activity under TC condition and no catalytic activity under LC condition for soot oxidation.

The effect of coexisting SOF on the soot oxidation with CeO_2-based catalysts was different from that with TiO_2-based catalysts. Under the TC condition, T_{max} values of PM-soot were lower than those of pure soot for all the catalysts. This can be explained by the occurrence of SOF oxidation with all the catalysts. As discussed for TiO_2-based catalysts, occurrence of SOF oxidation in SOF and soot mixture at lower temperature promoted the PM-soot oxidation at higher temperature possibly through the activation of surface of PM-soot. Under the LC condition, on the other hand, PM-soot was oxidized at higher temperature than pure soot. As discussed with Ag/TiO_2, loosening of PM/catalyst contact by thinning of simulated PM might prevail in the LC mixture with CeO_2-based catalysts.

Finally, influence of support materials on soot oxidation activity will be discussed with the results of TC mixture of simulated PM (Tables 1 and 2). CeO_2 was more active than TiO_2 as discussed in Section 3.2.1. T_{max} values with Ag/TiO_2 and Ag/CeO_2 were identical at 393 °C, indicating that Ag plays main role in soot oxidation. T_{max} values for Pt/TiO_2 and Pd/TiO_2 were 534 and 521 °C, and those for Pt/CeO_2 and Pd/CeO_2 were 434 and 446 °C. Since Pt and Pd exhibited weak catalytic activity under the condition, difference in T_{max} originated from that in the activity of support materials.

4. Conclusion

In this study, catalytic performance of TiO_2 and CeO_2 supported precious metal (Ag, Pt and Pd) catalysts for SOF and soot oxidation was investigated under both tight contact (TC) and loose contact (LC) conditions. Simulated PM was home-made from eicosane and carbon black as substitute of SOF and soot, respectively. Since laboratory tests of simulated PM have been scarcely reported, experimental methods and analysis of the TG/DTA/MS results were first investigated. Catalytic performance for the oxidation of SOF and soot in simulated PM depended on both metal species and supports. CeO_2 possessed inherent activity for both SOF and soot oxidation, while TiO_2 was nearly inactive for both reactions. For SOF oxidation which was independent of the contact condition, Pt was the most active species, followed by Pd and Ag. Soot oxidation under TC condition proceeded at lower temperature than that under LC condition, and Ag was far more active than Pt and Pd under both TC and LC conditions. Ag/CeO_2 was the most active soot oxidation catalyst among the catalysts investigated. The oxidation of soot was influenced by the coexisting SOF depending on catalytic materials and contact modes, and this was discussed in relation with the soot/catalyst contact condition and the activation of soot surface which is caused by desorption and oxidation of SOF taking place in advance of the soot oxidation.

Acknowledgement

The author (C.B. Lim) is grateful for financial assistance provided by the Global-Centre of Excellence in Novel Carbon Resource Sciences, Kyushu University.

References

[1] J.C. Summers, S. Van Houtte, D. Psaras, Appl. Catal. B 10 (1996) 139.
[2] R.H. Hammerle, D.A. Ketcher, R.W. Horrocks, G. Lepperhoff, G. Hüthwohl, B. Lüers, SAE Technical Paper Series, Paper Number 942043, 1994.
[3] H.S. Rosenkranz, Mutat. Res. 367 (1996) 65–72.
[4] J.G.M. Brandin, L.A.H. Andersson, C.U.I. Odenbrand, Catal. Today 4 (1989) 187–203.
[5] M. Ambrogio, G. Saracco, V. Specchia, Chem. Eng. Sci. 56 (2001) 1613–1621.
[6] D. Fino, P. Fino, G. Saracco, V. Specchia, Chem. Eng. Sci. 58 (2003) 951–958.
[7] J. Yang, M. Stewart, G. Maupin, D. Herling, A. Zelenyuk, Chem. Eng. Sci. 64 (2009) 1625–1634.
[8] D.J. Williams, J.W. Milne, S.M. Quigley, D.B. Roberts, Atmos. Environ. 23 (1989) 2647–2661.
[9] A. Robbat, N.P. Corso, P.J. Doherty, Anal. Chem. 58 (1986) 2078–2084.
[10] A. Durran, M. Carmona, J.M. Monteagudo, Chemosphere 56 (2004) 209–225.
[11] D. Fino, P. Fino, G. Saracco, V. Specchia, Chem. Eng. Sci. 57 (2002) 4955–4966.
[12] P. Ciambelli, V. Palma, P. Russo, S. Vaccaro, J. Mol. Catal. A 204–205 (2003) 673–681.
[13] G. Saracco, C. Badini, N. Russo, V. Specchia, Appl. Catal. B 21 (1999) 233–242.
[14] V.G. Milt, C.A. Querini, E.E. Miro, M.A. Ulla, J. Catal. 220 (2003) 424–432.
[15] P. Ciambelli, V. Palma, P. Russo, S. Vaccaro, Catal. Today 73 (2002) 363–370.
[16] P. Ciambelli, V. Palma, P. Russo, S. Vaccaro, Catal. Today 73 (2002) 363.
[17] H. An, C. Kilroy, P.J. McGinn, Catal. Today 98 (2004) 423.
[18] C. Badini, G. Saracco, V. Serra, V. Specchia, Appl. Catal. B: Environ. 18 (1998) 137.
[19] Y. Teraoka, K. Kanada, S. Kagawa, Appl. Catal. B: Environ. 34 (2001) 73.
[20] K. Wang, L. Qian, L. Zhang, H. Liu, Z. Yan, Catal. Today 158 (2010) 423–426.
[21] B. Zhao, R. Wang, X. Yang, Catal. Commun. 10 (2009) 1029–1033.
[22] X. Wu, R. Ran, D. Weng, Catal. Lett. 131 (2009) 494–499.
[23] E. Aneggi, J. Llorca, C. Leitenburg, G. Dolcetti, A. Trovarelli, Appl. Catal. B: Environ. 91 (2009) 489–498.
[24] K. Villani, R. Brosius, J.A. Martens, J. Catal. 236 (2005) 172–175.
[25] M. Machida, Y. Murata, K. Kishikawa, D. Zhang, K. Ikeue, Chem. Mater. 20 (2008) 4489–4494.
[26] K.-i. Shimizu, H. Kawachi, A. Satsuma, Appl. Catal. B: Environ. 96 (2010) 169–175.
[27] A.B. Lopez, K. Krishna, M. Makkee, J.A. Moulijn, Catal. Lett. 99 (2005) 3–4.
[28] I. Atribak, I.S. Basanez, A.B. Lopez, A.G. Garcia, J. Catal. 250 (2007) 75–84.
[29] I. Atribak, A.B. Lopez, A.G. Garcia, J. Catal. 259 (2008) 123–132.
[30] X. Wu, F. Lin, H. Xu, D. Weng, Appl. Catal. B: Environ. 96 (2010) 101–109.
[31] M. Dhakad, T. Mitshuhashi, S. Rayalu, P. Doggali, S. Bakardjiva, J. Subrt, D. Fino, H. Haneda, N. Labhsetwar, Catal. Today 132 (2008) 188–193.
[32] I. Atribak, A. Bueno-Lopez, A. Garcia-Garcia, J. Catal. 259 (2008) 123–132.
[33] X. Wu, Q. Liang, D. Weng, Z. Lu, Catal. Commun. 8 (2007) 2110–2114.
[34] H. Liu, H. Einaga, Y. Teraoka, unpublished results.